Geologia USP
Série Científica

DOI: 10.11606/issn.2316-9095.v19-148374

Revista do Instituto de Geociências - USP
Geol. USP, Sér. cient., São Paulo, v. 19, n. 3, p. 55-75, Setembro 2019

SHRIMP U-Pb zircon dating of Neoproterozoic granites from the easternmost São Roque Domain, Ribeira Belt

Datação U-Pb em zircão por SHRIMP de granitos Neoproterozoicos da porção oriental do Domínio São Roque, Faixa Ribeira

Ingrid Souto Maia Lamoso[1], Valdecir de Assis Janasi[1]
[1]Universidade de São Paulo - USP, Instituto de Geociências - IGc, Rua do Lago, 562, Butantã, CEP 05508-080, São Paulo, SP, BR
(ingridlamoso@gmail.com; vajanasi@usp.br)

Received on July 24, 2018; accepted on May 15, 2019

Abstract

Four granitic plutons from the easternmost portion of the São Roque Domain (SRD) were dated by U-Pb zircon SHRIMP; the results indicate that the peak of granitic magmatism was concentrated in a short interval (606–589 Ma), the same as in the central portion of the SRD. The two porphyritic biotite granites (Morro Azul and Imbiruçu) yield the oldest ages (respectively, 601.0 ± 4.9 Ma and 606.3 ± 4.8 Ma) and have inherited zircons with similar ages (~2.1–2.0 Ga), but are not comagmatic. The Morro Azul granite has geochemical signature similar to other high-K calc-alkaline (HKCA) granites from the SRD, while the Imbiruçu granite has much higher Sr/Zr and other chemical features that demand different sources. Other two dated samples are very different from each other and from the HKCA granites. The age of the Morro do Pão tonalite (589.1 ± 5.5 Ma) indicates that, in spite of its more deformed character, it is younger; a similar value, although with large uncertainty, is shown by the Serra dos Índios peraluminous leucogranite (593 ± 12 Ma). Our analytic data combined with field relationships suggest that soon after the main episode of HKCA magmatism, the SRD witnessed the emplacement of granites of varied composition forming small bodies that recorded deformation associated with transcurrent tectonics.

Keywords: Geochronology; Geochemistry; São Roque Domain; Granite magmatism; SHRIMP; Ribeira Belt.

Resumo

Foram obtidas, por (SHRIMP), idades U-Pb em cristais de zircão de quatro plútons graníticos da porção mais oriental do Domínio São Roque. Os resultados indicam que o pico da granitogênese foi concentrado em um curto intervalo de tempo (606–589 Ma), o mesmo daquele de colocação dos granitos na porção central do Domínio São Roque. Os dois biotita granitos porfiríticos (Morro Azul e Imbiruçu) apresentam as idades mais antigas obtidas (601.0 ± 4.9 Ma e 606.3 ± 4.8 Ma, respectivamente), além de possuírem cristais de zircão com núcleos herdados de mesma idade (~2.1–2.0 Ga), contudo estes não são comagmáticos. O maciço Morro Azul tem assinatura geoquímica similar a outros granitos cálcio-alcalinos de alto potássio típicos do Domínio São Roque, enquanto o maciço Imbiruçu possui uma razão Sr/Zr muito maior que estes, assim como outras características químicas, o que implica fontes distintas. Outras duas ocorrências datadas são muito diferentes umas das outras e dos granitos cálcio-alcalinos de alto potássio. A idade do tonalito Morro do Pão (589.1 ± 5.5 Ma) indica que este é mais jovem, apesar de possuir caráter mais deformado. Valor similar, apesar da grande incerteza, é apresentado pelo leucogranito peraluminoso Serra dos Índios (593 ± 12 Ma). Isso sugere que, logo após o principal episódio de magmatismo de alto potássio, o Domínio São Roque testemunhou a colocação de granitos com uma variedade composicional muito ampla, formando pequenos corpos que registram deformação associada com tectônica transcorrente.

Palavras-chave: Geocronologia; Geoquímica; Domínio São Roque; Magmatismo granítico; SHRIMP; Faixa Ribeira.

INTRODUCTION

Recent widespread usage of U-Pb zircon dating by *in situ* techniques, especially Sensitive High Resolution Ion Micro-Probe (SHRIMP), is improving significantly the geochronology of Neoproterozoic granitic magmatism from SE Brazil. The ability to quickly process analyses is certainly important, and more than compensates in many cases the lower precision (2σ~5–6 Ma for ages ~600 Ma; Sato et al., 2014) as compared to ID-TIMS. Equally important, however, is that the spatial resolution of ~20 μm allows to avoid sites of loss of lead (e.g., fractures, inclusions of other minerals or areas subject to post-magmatic textural modification) and also, in a number of cases, circumvent small inherited zircon nuclei which, if included in the analysis, would result in ages greater than the true age of magmatic crystallization. One of our recent systematic dating programs (Janasi et al., 2016) revealed that the age of the high-K calc-alkaline (HKCA) magmatism, which formed the most voluminous plutons intruding the low- to medium- grade meta-volcano-sedimentary sequences of São Roque Domain (SRD), seems confined to a small interval (~605–595 Ma), which is ~30 Ma younger than previously admitted for these rocks, on the basis of U-Pb TIMS dating (Töpfner, 1996). This discrepancy was tentatively attributed to inadvertent inclusion of small inherited nuclei in the multigrain zircon fractions used in the TIMS analyses. In fact, tiny inclusions of inherited zircon are common in crystals from many granite samples from SRD, and are also present in the samples dated by Töpfner (1996).

Voluminous granitic magmatism comprising a wide variety of types (Campos Neto et al., 1983) is present in the easternmost part of SRD, east of the area studied by Janasi et al. (2016). Previous work by Ragatky (1998) and Ragatky et al. (2013) brought important information on the petrography and geochemistry of these granites, which include, along with porphyritic biotite granites that are very similar to the typical HKCA granites from the central SRD (e.g., the Morro Azul and Imbiruçu granites), several elongated plutons with widely varied composition, from tonalites (Morro do Pão suite) to leucogranites (Serra dos Índios suite). Moreover, Nd isotope results revealed that part of these occurrences (e.g., Imbiruçu, Morro do Pão) are more radiogenic (and thus have less negative eNd_t) compared to all known granites from the rest of the domain, implying different sources. However, analytical limitations at that time did not allow reliable ages of any of these plutons to be obtained by the methods employed, i.e., whole-rock Rb-Sr and U-Pb zircon TIMS.

The present work, therefore, was set to obtain precise ages of four of the most expressive granite occurrences of the easternmost part of SRD using the SHRIMP technique for U-Pb zircon dating. Petrographic and geochemical analyses were obtained to characterize each of these occurrences, and select the best samples. Besides the new age determinations, which result in a more complete geochronological panorama of the granite magmatism in the SRD, our geochemical data, in parallel with dating of inherited zircon crystals, also bring important information which are useful to investigate the petrogenesis of these granites.

GEOLOGICAL SETTING

Ribeira Belt is part of Mantiqueira Structural Province (Almeida et al., 1981), which extends from southern Bahia to Uruguay along the coastal region of South America. SRD, one of the several fault-bounded blocks in which Ribeira Belt is divided (Figure 1), hosts meta-volcano-sedimentary sequences of dominantly Statherian-Calymmian ages (Hackspacher et al., 2000; Henrique-Pinto et al., 2018; Juliani et al., 2000). A study of sedimentary provenance in SRD metasandstones indicates a predominance of Paleoproterozoic (~2.2–2.1 Ga) and Archean (2.7–2.4 Ga) sources (Henrique-Pinto et al., 2015).

SRD is bordered to the north by Socorro-Guaxupé Nappe (SGN), an allochtonous high-grade terrane that exposes a large (~20 km) vertical section of the Neoproterozoic crust (Campos Neto, 2000) and to the south by Embu Terrane, dominated by Neoproterozoic meta-volcano-sedimentary sequences with an Archean-Paleoproterozoic basement (Campanha et al., 2019; Duffles et al., 2016).

Granitic rocks from the SRD occur as a series of plutons whose shapes are often strongly controlled by NE-directed transcurrent shear zones (Figure 2), indicating that their emplacement was contemporaneous with strike-slip tectonics.

The largest plutons are mostly constituted by porphyritic biotite monzogranites to granodiorites/quartz monzonites with 2-4 cm K-feldspar megacrysts set in a medium to coarse-grained matrix. The metaluminous character of these granites is indicated by the presence of abundant accessory titanite; hornblende is present in granite varieties with higher proportions of mafic minerals, and may be absent in some plutons. Chemically, they are SiO_2-poor, often straddling the limit between acid and intermediate rocks (64–68 wt.%SiO_2), have relatively high mg# (35–45) and high K/Na values, and can be described as HKCA granites. Other typical geochemical features are fractionated rare earth elements (REE) patterns lacking significant Eu negative anomaly, high contents of LILE (Ba = 1,000–2,000 ppm; Sr = 600–1,000 ppm), and high Sr/Y (often > 30) (Ragatky, 1998; Ragatky et al., 2003). A contribution from contemporaneous mafic magmatism is evident in some occurrences, as scattered mafic synplutonic dykes and mafic microgranular enclaves. Often more evident are evidences of contamination by assimilation of metasedimentary rocks, which may appear as xenoliths or strongly modified mica-rich enclaves (Janasi et al., 2016).

MATERIALS AND METHODS

Fieldwork and petrography

Fieldwork campaigns were made to identify field relations between the different granite types and collect samples for laboratory work. Measurements of absolute magnetic susceptibility were made in fresh surfaces using a portable Exploranium, model KT-9 device. Measurements were done in the *pin* mode and register the magnetic susceptibility up to a depth of ~20mm with errors in the order of 1%. The measured values correspond to averages of ten measurements in a homogeneous restricted area (up to 1 m^2) of each outcrop.

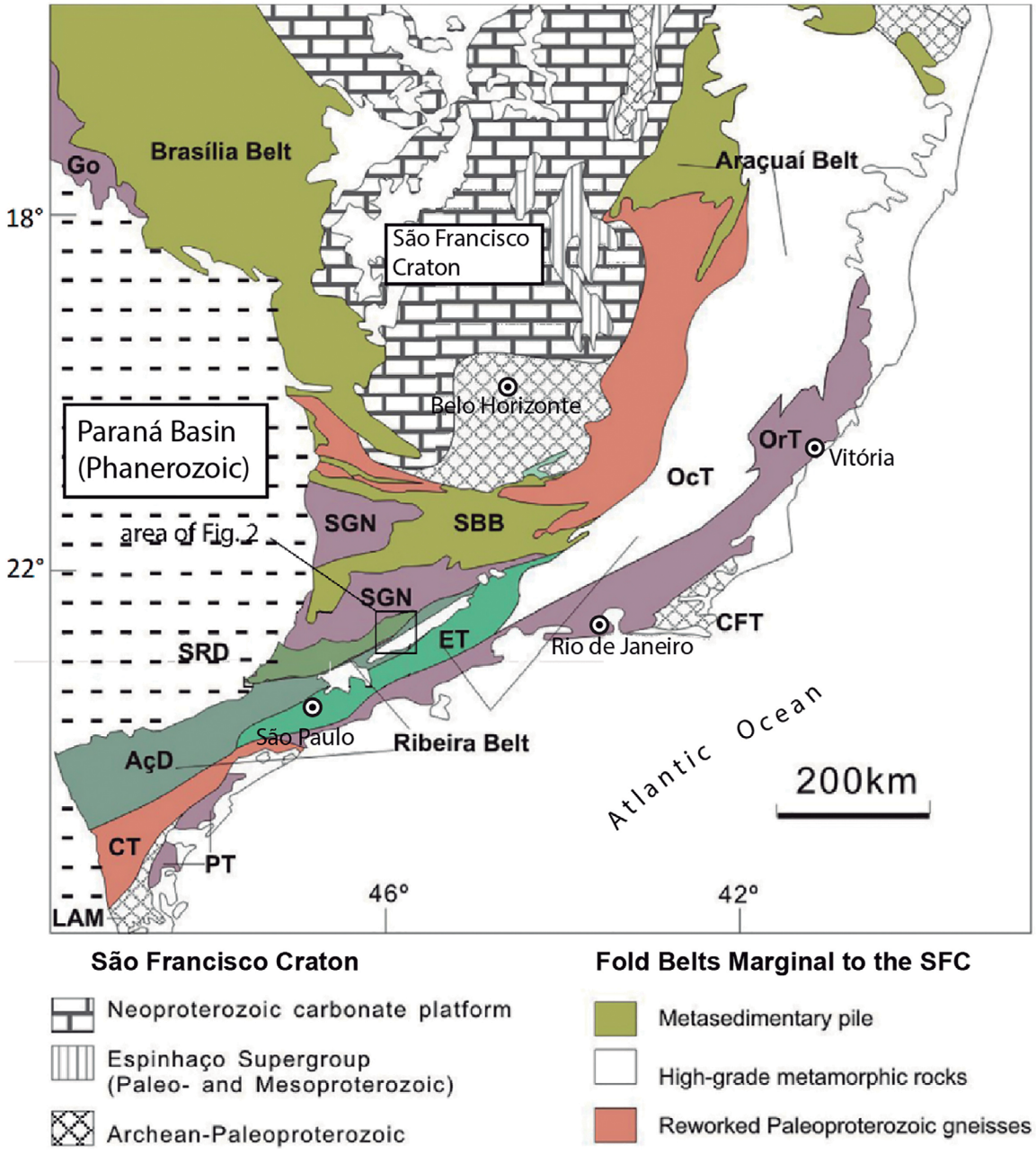

Source: Janasi et al. (2016); modified from Campos Neto et al. (2010).
AçD: Açungui Domain; CFT: Cabo Frio Terrane; CT: Curitiba Terrane; ET: Embu Terrane; Go: Goiás Magmatic Arc; LAM: Luiz Alves Microplate; OcT: Ocidental Terrane; OrT: Oriental Terrane; PT: Paraná Terrain; SBB: South Brasília Belt; SGN: Socorro-Guaxupé Nappe; SRD: São Roque Domain.

Figure 1. Tectonic framework of SE Brazil with location of the São Roque Domain in the Ribeira Belt.

Samples from four different plutons (Morro Azul — MA, Imbiruçu — IMB, Morro do Pão — MP, and Serra dos Índios — SI) were collected for zircon U/Pb study dating by SHRIMP. The Universal Transverse Mercator (UTM) coordinates of all analyzed samples in this study are listed in Tables 1 and 2.

Sample IGT-02A corresponds to a porphyritic biotite monzogranite with several mafic microgranular enclaves typical of the Morro Azul granite and was collected in a quarry approximately 1.5 km northwest of Igaratá.

Sample IGT-23 is a typical porphyritic biotite monzogranite of the Imbiruçu pluton and was collected in a roadcut outcrop where mafic microgranular enclaves are abundant. This sample belongs to the most mafic variety of IMB granite (see Table 1).

Sample IGT-13 corresponds to the most primitive (more mafic-rich) sample of Morro do Pão tonalite and was collected in an outcrop close to the Jucá Carvalho road, 17 km northeast from Igaratá.

Sample IGT-19 is a muscovite-bearing leucogranite of Serra dos Índios massif collected on the Guirra Road, 25 km northeast of Igaratá. The sample has abundant secondary minerals (pervasive sericite alteration of feldspars and secondary muscovite).

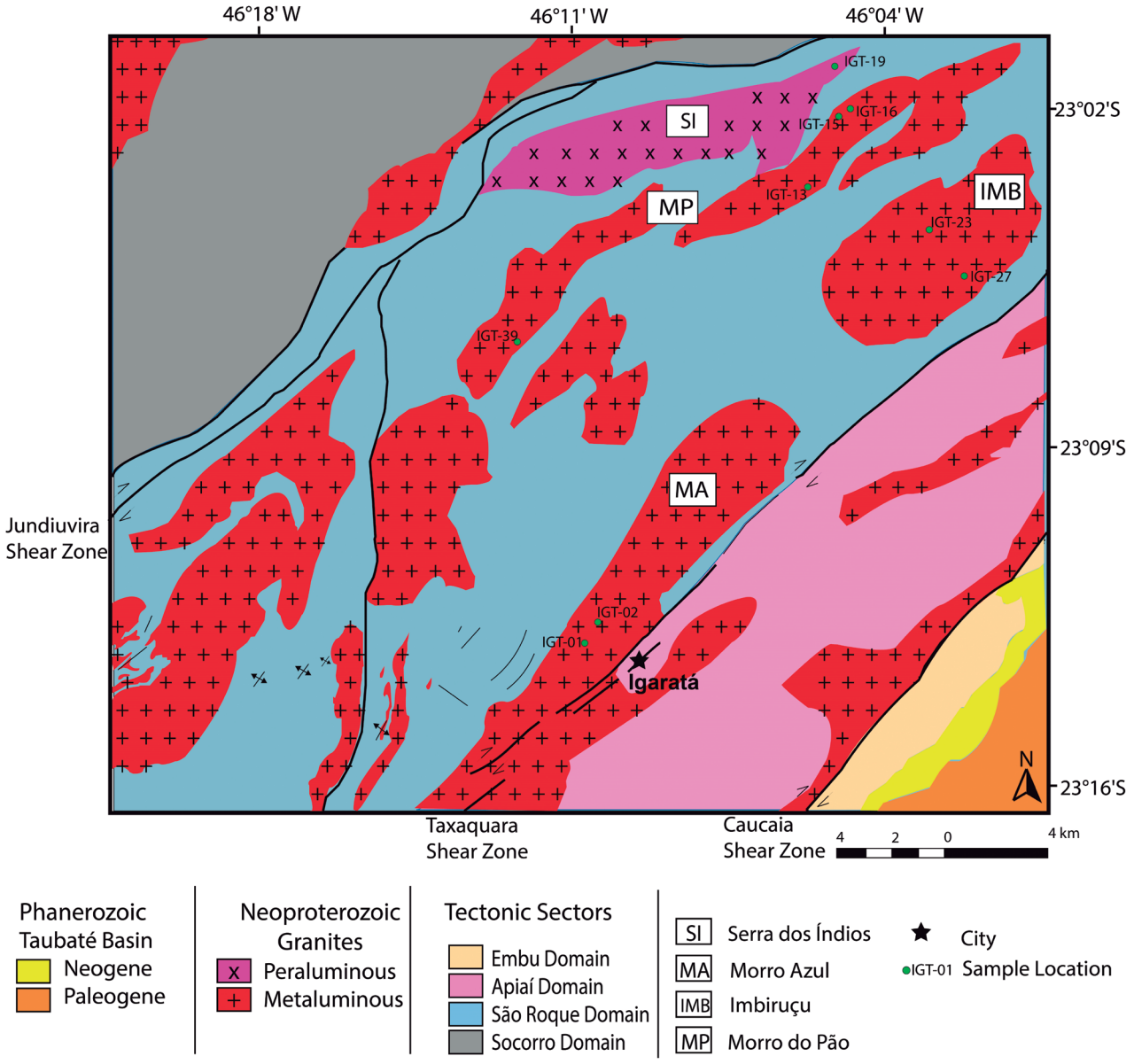

Source: modified from Campos Neto et al. (1983) and Janasi et al. (2016).

Figure 2. Geological sketch of the eastern part of São Roque Domain, showing the granites studied in this research.

Whole-rock major and trace-element analyses

X-ray Fluorescence was used to determine the major, minor and trace elements in whole rock samples. Large samples typically weighing 6–8 kg were broken into pieces of about 3–5 cm using hammer or hydraulic press, and then were crushed to fragments with an average size of 1.5 cm with a jaw breaker of Mn-steel. The material was then split in a cross-type Jones splitter, yielding 100–150 g sub-samples representative of the starting material. Sub-samples were then milled on a Pulverisette-type planetary agate mill for 15 minutes, which is usually enough to reach a particle size smaller than 200 mesh.

Analyses were performed in a PANalytical AXIOS MAX Advanced spectrometer at the NAP-Geonalitica, Instituto de Geociências, Universidade de São Paulo, Brazil, following the protocol described in Mori et al. (1999). Major and minor elements were analyzed from molten tablets obtained from a mixture of 1 g sample and 9 g of spectroscopic grade lithium tetra and metaborate at 1,100–1,200ºC in a platinum crucible, using a Claisse fusion machine. Trace elements were analyzed from pressed pellets obtained from homogenization of the pulverized sample (previously micronized in a McCrone Micronizer) and pressing to 30 ton with wax. Analytical quality was controlled using a reference material granite JG-1a from Geological Survey of Japan as an unknown sample, and duplicated samples. The values obtained are within 2σ of the certified values, and the duplicated samples within 1% of variation.

Zircon concentration, mounting and cathodoluminescence study

The separation and concentration of zircon grains consist of crushing, grinding, sieving, vibrating table, electromagnetic separation, heavy liquids and, finally, manual picking. The routine used at CPGeo is described by Sato et al. (2014) and consists of the following steps:

- rock samples (0.5 to 3 kg) are crushed in a jaw crusher;
- crushed material is screened to separate a fraction of 100–250 mesh particle size, using a disk mill and a battery of sieves;
- the separated fraction is taken to a vibratory table to concentrate heavy minerals;
- magnetic minerals are removed with a hand magnet;
- minerals with different magnetic susceptibilities are concentrated in a Frantz-type magnetic separator, by varying the inclination and the intensity of the electromagnetic field;
- the least magnetic fractions are passed successively into bromoform (d = 2.85 g/cm^3) and methylene iodide (d = 3.2 g/cm^3) to further concentrate the heavy minerals of interest.

Any remaining sulfides present in the concentrates are eliminated with HCl or HNO_3. About 50-100 zircon grains are separated by hand picking with the aid of a magnifying microscope, and then mounted on double sided adhesive tape and embedded in epoxy-type resin. The mount is then polished to expose the fresh surface of the grain trapped in the resin. A previous study of cathodoluminescence (CL) of each of the samples was necessary to choose the proper position of the spot during the *in situ* analyses by SHRIMP. After a thin layer of gold cover (2–3 mm) was added to the mounts, these images were obtained in a FEI Quanta 250 SEM spectrometer with a XMAX CL detector (Oxford Instruments). Operating conditions were: high voltage, 15 kV, distance, 16.9-17 mm, PMD detector, range of magnification, 95-250x.

Table 1. Values of magnetic susceptibility obtained in the fieldwork for the studied plutons.

Pluton	Point	UTM (Zone 23K)	Magnetic susceptibility (× 10^{-3} SI)
Morro Azul	IGT-01	7433967N; 380036E	0.35
	IGT-02	7434484N; 380471E	0.42; 0.51
	IGT-08	7436023N; 382007E	0.31
	IGT-09	7437226N; 382206E	0.42
Imbiruçu	IGT-22	7448508N; 391903E	7.11
	IGT-23	7447862N; 392284E	7.00; 5.24
	IGT-24	7446307N; 391587E	4.51
	IGT-25	7446034N; 391932E	4.20
	IGT-27	7446370N; 394202E	4.81
	IGT-28	7447205N; 392762E	4.48
	IGT-30	7446178N; 389551E	5.00; 4.69
Morro do Pão	IGT-13	7449479N; 386787E	0.66; 0.67
	IGT-15	7452040N; 388711E	19.8; 28.0
	IGT-16	7452191N; 389113E	2.03; 3.03
	IGT-39	7442933N; 376034E	20.8
Serra dos Índios	IGT-19	7455650N; 392132E	0.06

U-Pb geochronology by SHRIMP

U-Pb zircon dating was performed in the SHRIMP-IIe equipment installed at CPGeo, Instituto de Geociências, Universidade de São Paulo. SHRIMP is a mass spectrometer coupled to a high-resolution ion microprobe that uses a collimated and accelerated beam of primary ions (O_2) to reach a target where secondary ions are generated from 30 mm spots. The secondary ions are accelerated through the equipment and the isotopes generated by the sample, $^{254}UO^+$, $^{206}Pb^+$, $^{207}Pb^+$, $^{208}Pb^+$, $^{238}U^+$ and $^{254}ThO^+$ and $^{196}Zr2O^+$, are measured successively. The corrections required by the

Table 2. Whole-rock geochemistry data for major (% in weight), minor and trace-elements (ppm) by X-ray fluorescence (XRF) for Morro Azul (MA) and Imbiruçu (IMB) granites. S and Cl display values below the quantification limit for all samples (< 550 and < 500, respectively).

	Morro Azul			Imbiruçu		Morro do Pão				Serra dos Índios
	IGT-01	IGT-02A	IGT-02C	IGT-23	IGT-27	IGT-13	IGT-15	IGT-16	IGT-39	IGT-19
UTM S: 23K	7433967 380036	7434484 380471	7434484 380471	7447862 392284	7446370 394202	7449479 386787	7452040 388711	7452191 389113	7442933 376034	7455650 392132
SiO_2	62.75	67.47	61.26	66.20	71.01	53.72	56.87	62.53	57.51	71.36
TiO_2	1.197	1.014	1.376	0.659	0.362	1.864	1.87	1.288	1.987	0.212
Al_2O_3	15.66	13.13	15.47	15.67	14.41	16.93	16.79	16.28	15.51	16.04
Fe_2O_3	6.45	5.73	6.47	4.00	2.33	8.52	7.86	5.95	7.80	1.35
MnO	0.084	0.078	0.086	0.059	0.046	0.110	0.102	0.079	0.109	0.022
MgO	1.99	1.71	2.18	1.37	0.75	3.49	3.15	2.14	2.73	0.32
CaO	3.63	2.79	4.06	2.77	1.83	5.61	5.49	3.74	5.61	1.01
Na_2O	3.28	2.72	3.56	3.62	3.81	3.51	3.80	3.51	3.01	3.19
K_2O	3.8	3.44	3.1	4.43	4.13	3.59	3.14	3.94	3.29	4.63
P_2O_5	0.436	0.381	0.539	0.293	0.160	0.845	0.720	0.517	0.581	0.057
LOI	0.83	0.61	0.74	0.57	0.62	0.74	0.69	0.58	0.74	2.32
Total	100.11	99.07	98.84	99.64	99.46	98.93	100.48	100.55	98.88	100.51
Rb	137	152	139	139	147	112	95	138	125	263
Ba	1188	783	1042	1583	953	1495	1224	1487	1290	489
Sr	492	340	495	887	628	786	998	676	576	190
Ni	16	15	16	< 5	< 5	25	23	14	9	< 5
Cr	25	21	26	16	< 13	51	40	37	17	< 13
V	87	75	82	54	29	132	130	85	146	12
Cu	17	13	20	11	5	26	23	18	20	19
Pb	14	15	10	15	21	16	14	13	20	59
Nb	23	22	29	11	< 9	26	25	20	26	10
Zr	427	414	448	264	171	418	151	429	457	148
Y	21	19	22	14	9	23	20	19	22	6
Th	12	9	12	10	< 7	17	7	14	12	14
U	9	7	7	7	3	10	10	6	9	3
La	80	62	115	76	56	113	72	118	114	37
Ce	145	111	223	121	86	175	130	248	197	53
Nd	59	40	74	54	27	58	57	73	85	19
Co	14	12	15	8	< 6	23	20	15	20	< 6
Ga	22	19	23	21	20	23	22	24	22	28
Sc	< 14	< 14	< 14	< 14	< 14	15	15	< 14	16	< 14
Zn	89	80	96	79	51	109	118	101	108	61
F	1,530	1,552	1,872	1,227	871	1,279	1,451	2,091	2,314	905
A/CNK	0.97	0.99	0.93	0.99	1.02	0.85	0.86	0.97	0.83	1.33
A/NK	1.65	1.60	1.68	1.46	1.34	1.75	1.74	1.62	1.82	1.56
mg#	37.93	37.15	40.02	40.41	38.93	44.79	44.25	41.60	40.94	31.95

MA: Morro Azul; IMB: Imbiruçu; MP: Morro do Pão; SI: Serra dos Índios.

technique were made by the analyses of unknown and reference materials with known isotopic ratios (matrix-matched) for determining specific calibration factors (Black et al., 2004). 12–16 spot analyses from each of the unknown zircon samples were performed according to the method described in Sato et al. (2014). During the run, every five determinations analyzed the Temora-2 reference material (estimated age 416.78 ± 0.33 Ma; Black et al., 2004) which is used as $^{206}Pb/^{238}U$ age reference, and for calculation of common Pb correction factors and fractionation factors. Common lead corrections use ^{204}Pb according to Stacey and Kramers (1975). Reference material SL13 (238 ppm) was used as U composition reference. Data were reduced with SQUID 1.6 software (Ludwig, 2009) and ISOPLOT 4 (Ludwig, 2003) was used for treatment of data to estimate ages and generate diagrams.

FIELD ASPECTS AND PETROGRAPHY

Morro Azul Granite

The MA granite has an elongated shape concordant with the main regional NE direction (23 km length × up to 4 km width; total area ~45 km^2), and is located at the southernmost part of the SRD, being affected by the Taxaquara Shear Zone (Figure 2). The main rock type is a mafic-rich (color index, CI~15) porphyritic biotite monzogranite with ~30% alkali feldspar megacrysts (average 3 × 1 cm, with rectlinear outlines, most undeformed) set in a fine to medium-grained inequigranular matrix (0.3–4 mm). It is hosted in a metasedimentary sequence composed mainly of muscovite-schists with porphyroblasts of garnet, interleaved with quartzite.

The foliation is defined mainly by oriented biotite crystals as well as by stretched feldspar and quartz crystals in the matrix. Alkali feldspar megacrysts are poikilitic, with inclusions of primary minerals (plagioclase, quartz, biotite, titanite) and products of alteration (muscovite, chlorite, calcite). The typical MA granite has quartz (19–30%), plagioclase (22–30%), alkali feldspar (25–38%), biotite (10–14%), muscovite (0–4%), opaque minerals (< 1–1%), chlorite (< 1–2%), and accessory allanite, apatite, epidote, tourmaline, zircon and carbonate. Matrix quartz and feldspar show microgranular textures; larger quartz crystals may also occur as mosaic. Euhedral to subhedral crystals of opaque minerals are usually mantled by titanite.

Dark (CI~25) microgranular enclaves (Figure 3C) are abundant in nearly all outcrops of the MA granite, and have a tonalitic-granodioritic composition, and a foliated structure mainly defined by orientation of biotite. They have varied forms, from oval to subcircular, reflecting different degrees of deformation, and are usually composed by plagioclase (40–46%), quartz (22–24%), biotite (~20%), alkali feldspar (2–4%), titanite (up to 4%), muscovite (1–2%) and opaque minerals (1%).

Low values of magnetic susceptibility (~ 0.3–0.5 × 10^{-3} SI; Table 1) are typical of both granites and enclaves, reflecting the absence of magnetite.

Imbiruçu Granite

The IMB Granite has an ellipsoidal shape in plant, elongated in the NE direction (approximately 10 km length × 4.5 km width; total area ~42 km^2), and is located NE of MA granite; it is intrusive into low- to medium-grade metasedimentary rocks of the São Roque Group (Figure 2). There are two different IMB varieties (Figures 3 and 4): the predominant one is texturally similar to the MA granite (a porphyritic biotite monzogranite with CI ~15) while the least expressive variety has lower CI (~8) and occurs in the SE portion of the pluton. The texture and mineralogy of both varieties are quite similar, but the subordinate variety tends to syenogranitic compositions.

Compared to MA, alkali feldspar megacrysts in the IMB granites are less abundant (~20%) and smaller (average 2 cm long and 0.7 cm wide, with rectilinear outlines, undeformed to slightly deformed). These megacrysts are sometimes parallel to the foliation, which is marked mainly by biotite orientation. IMB varieties have relatively high contents (up to 3%) of epidote, and the opaque minerals are usually idiomorphic and associated to biotite; mantled textures with titanite are absent to rare.

Mafic microgranular enclaves (CI = 26–37) are common, but less abundant than in MA, and commonly show a foliation defined by oriented biotite. Their composition is predominantly granodioritic and, to a lesser extent, monzogranitic. The enclaves are inequigranular fine-grained (~0.2–0.6 mm) and composed by biotite, plagioclase, alkali feldspar, quartz, titanite, and minor amounts of muscovite, chlorite, epidote, apatite and opaque minerals in different proportions. Occasionally, they include K-feldspar from the host granite (Figure 3D).

Values of magnetic susceptibility in both IMB granites and enclaves are consistently higher than those of MA, varying between 4.2 and 7.1 × 10^{-3} SI (Table 1).

Morro do Pão suite

The MP suite consists of two main bodies (with areas ~21 and 10 km^2) elongated in the N60–70E direction located in the northern portion of SRD in the region shown in Figure 2. The original definition (Campos Neto et al., 1983) included both mafic (tonalite) and more felsic (granitic) compositions. The tonalites, studied here, have high CI = 25–30, with the mafic minerals (mostly biotite and hornblende) defining the foliated structure.

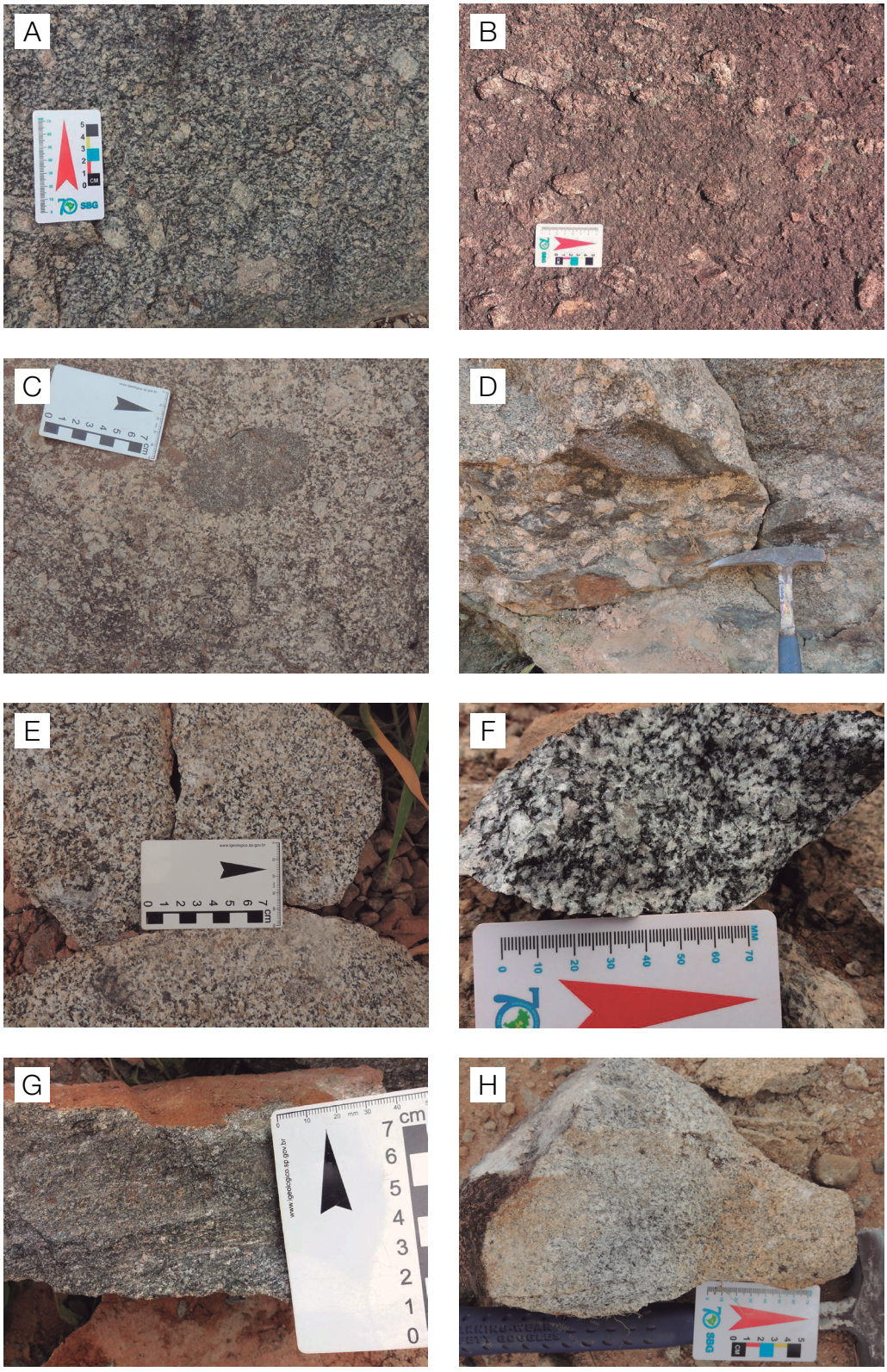

MA: Morro Azul; IMB: Imbiruçu; MP: Morro do Pão; SI: Serra dos Índios.

Figure 3. Field photographs of typical varieties of studied granites. (A) and (B) MA granite; (C) mafic microgranular enclave within a MA granite; (D) mafic microgranular enclaves with included K-feldspar megacrysts in IMB granite; (E) more felsic variety of IMB granite; (F) more mafic and common variety of IMB granite; (G) MP tonalite; (H) SI leucogranite.

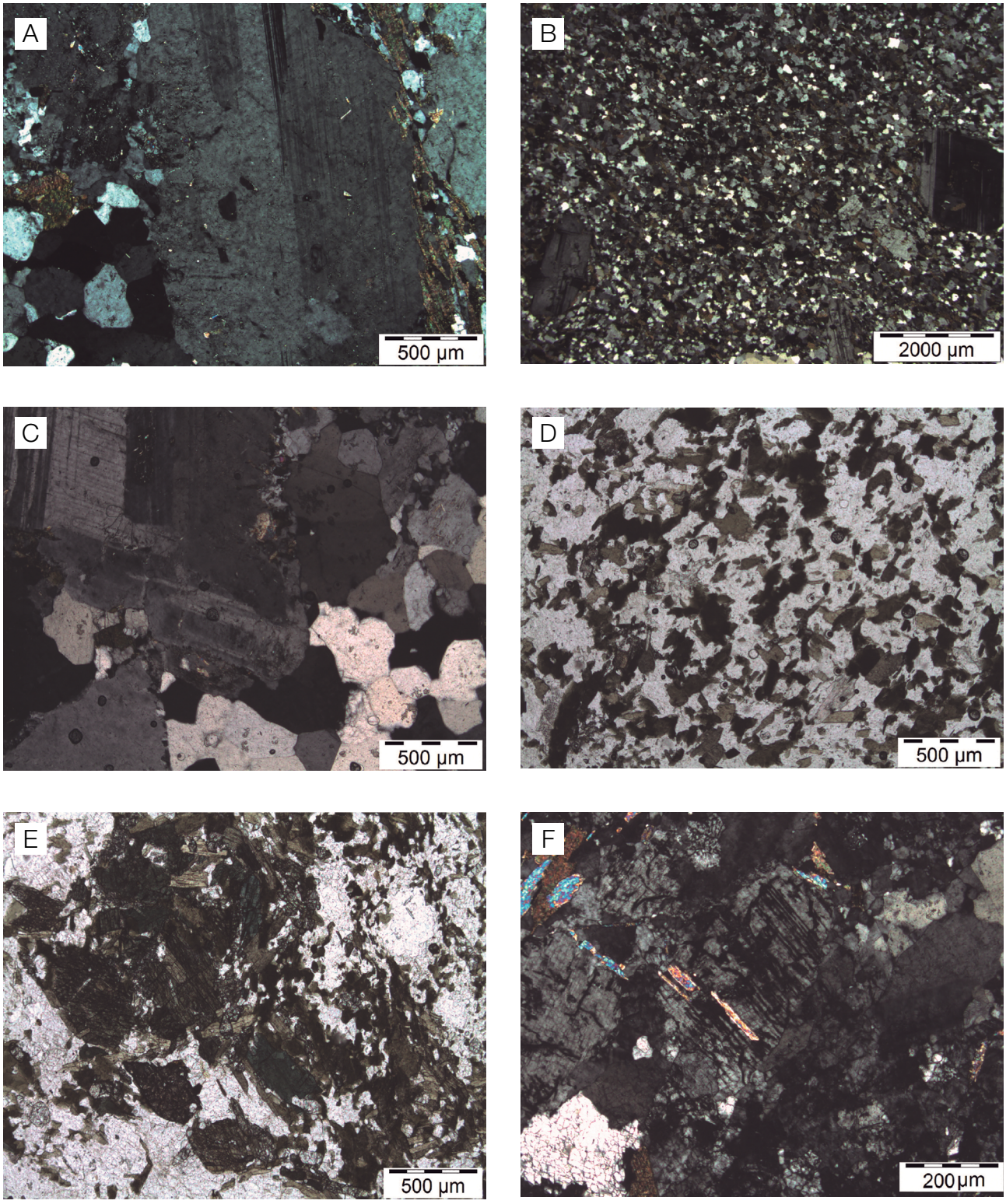

MA: Morro Azul; IMB: Imbiruçu; MP: Morro do Pão; SI: Serra dos Índios.

Figure 4. Photomicrographs in transmitted light microscope. (A) MA granite; (B) Microgranular mafic enclave from MA granite; (C) IMB granite; (D) Microgranular mafic enclave from IMB granite; (E) MP tonalite; (F) SI leucogranite showing secondary muscovite related to k-feldspar.

MP tonalites are inequigranular fine to medium-grained (0.4–2.5 mm), and are composed by plagioclase (~45%), quartz (25–31%), biotite (13–20%), alkali feldspar (2–5%), hornblende (2–5%), epidote, titanite and accessory opaque minerals, apatite, zircon, and tourmaline. Opaque minerals can be mantled by titanite, and hornblende is often surrounded by biotite (Figure 4). Quartz shows microgranular and mosaic textures.

The magnetic susceptibility values are widely varied in different expositions of the MP tonalite, from 0.66 × 10^{-3} to 28 × 10^{-3} SI (Table 1).

Serra dos Índios leucogranites

The SI granites as defined by Campos Neto et al. (1983) occur as very elongate bodies in the N75ºE direction, with a high degree of deformation, and intercalated with lenses of metamorphic rocks in a region of difficult access in the northern part of SRD in Figure 2. The sample collected for this study is a foliated white-colored granite with very low CI (3-5) and low (~5%) proportion of alkali feldspar megacrysts (average 1.5 × 0.5 cm) in a medium-grained inequigranular matrix (0.6–2.0 mm).

The rock has its primary mineralogy (Figure 4) composed by quartz (~35%), alkali-feldspar (~45%), plagioclase (~15%), biotite (~4%) and opaque minerals (< 1%). Quartz usually occurs in *ribbons* defining the foliation, that can also be defined by stretched feldspar crystals. Both quartz and feldspar may occur in mosaic and microgranular textures. Secondary muscovite (~4%) and pervasive sericite alteration of plagioclase are abundant.

SI granites have very low magnetic susceptibility (0.06 × 10^{-3} SI), as indicated in Table 1.

WHOLE-ROCK GEOCHEMISTRY

Whole-rock geochemical data of major, minor and trace elements were obtained for representative samples of the studied granites. The number of analyzed samples is relatively small and clearly insufficient to characterize the internal diversity of each occurrence, so the purpose of our analytical work is not to explore the geochemical evolution of the individual occurrences, but to characterize their general geochemical features, which is useful to insert the samples that were chosen for U-Pb dating within the geochemical variation identified in the plutons, as defined in previous works.

In fact, significant amount of geochemical results for these granites is available in the literature (Ragatky, 1998; Ragatky et al., 2003). In the following evaluation of the geochemical data, our results are used in conjunction with these previous data; it allows to evaluate if the chosen samples are representative of the studied plutons, and additionally to check the consistency of data obtained in different laboratories.

As shown in Table 2, MA, MP and the less differentiated IMB samples (IGT-23) have metaluminous character, while more felsic IMB sample (IGT-17) is slightly peraluminous, and the SI sample is strongly peraluminous (A/CNK = 1.33; Figure 5).

The mg# parameter [calculated as 100*(MgO/(MgO + FeO) in molar proportions; all Fe as FeO] is important indicator of differentiation and, at similar SiO_2 contents, may be sensitive to the state of magma oxidation. The lowest mg# is shown by the fractionated peraluminous SI granite. For MA, IMB and MP, there is a good correlation between the SiO_2 content and mg#, with higher mg# (~ 41–45) associated with the more mafic MP. The mg# values for MA and IMB are similar, with a slightly higher value for the MA mafic microgranular enclave (IGT-02C) and a slightly lower value for the most differentiated IMB sample (IGT-27). The slightly higher mg# of IMB compared to MA at similar SiO_2 contents is consistent with a more reduced character of MA, already suggested by its very low magnetic susceptibility.

Binary variation diagrams show that the compositions of IMB and MA show important overlap for several elements (e.g., Rb, MnO, Th, CaO, P_2O_5 and MgO) (Figures 6 and 7). However, for similar degrees of differentiation, MA shows lower contents of K, Al, Ba, Sr (elements present in feldspar) and higher contents of Fe, Ti, Mn, P, Zr (elements present in mafic and accessory minerals). The most remarkable difference is shown by Sr and Zr and is further evidenced comparing the Sr/Zr ratios: 0.8–1.2 in Morro Azul and 3.3–3.7 in Imbiruçu.

The MP tonalites are the most primitive of all studied samples (54–62 wt.% SiO_2, with the highest Fe_2O_3, MgO, MnO and CaO contents). The four samples analyzed, however, do not follow a single trend (Figures 6 and 7).

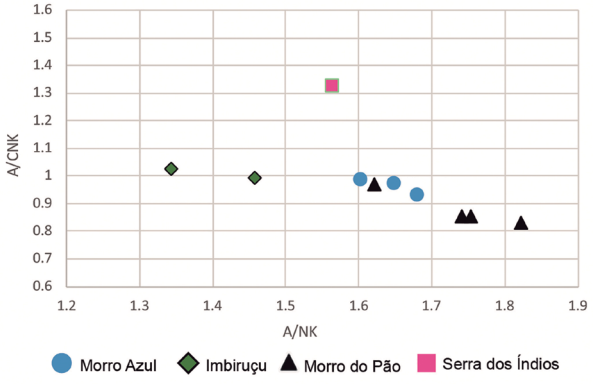

MA: Morro Azul; IMB: Imbiruçu; MP: Morro do Pão; SI: Serra dos Índios.

Figure 5. A/CNK *versus* A/NK diagram for MA, IMB, MP and SI granites, from samples studied in this research.

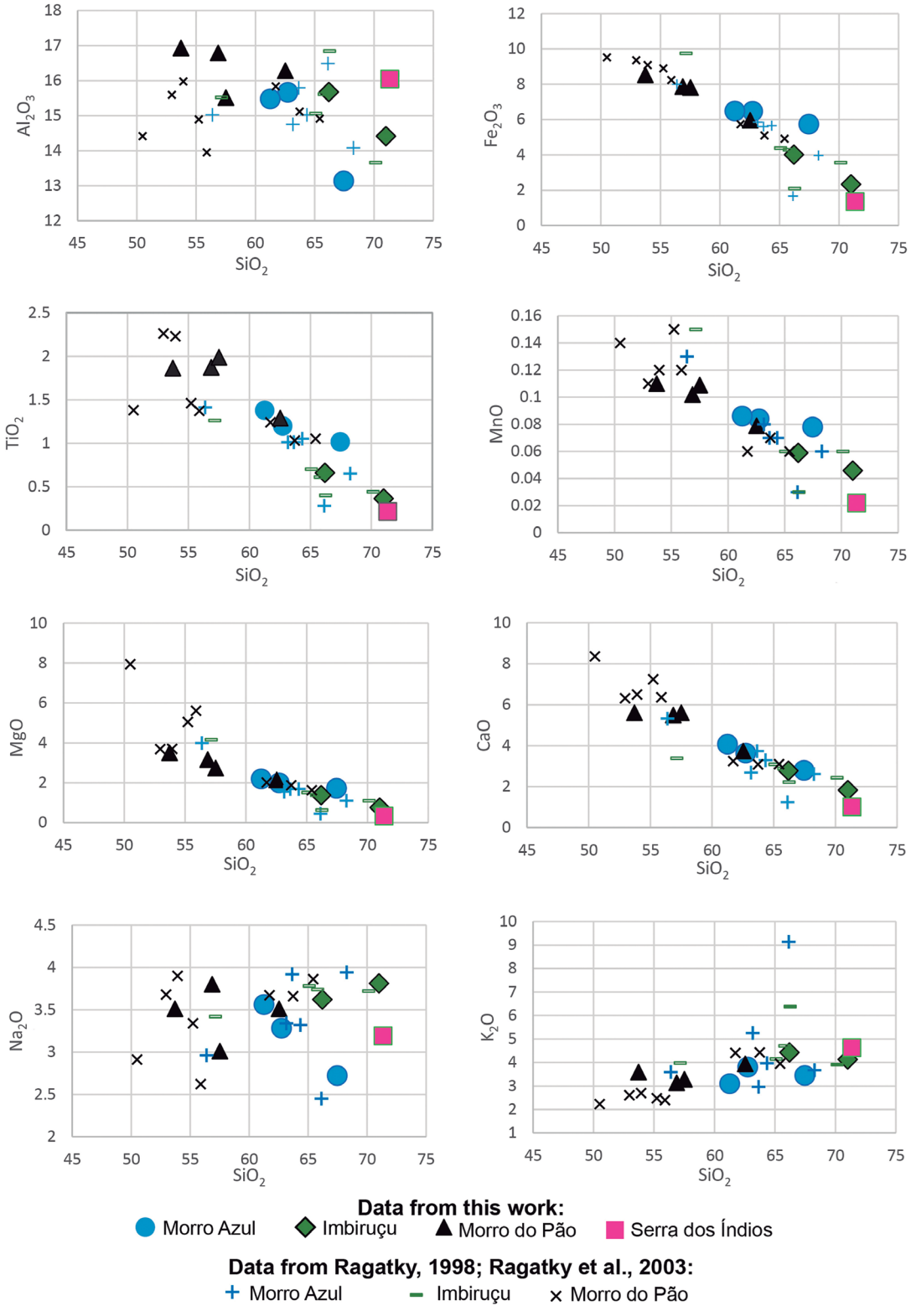

Source: from Ragatky (1998) and Ragatky et al. (2003).
MA: Morro Azul; IMB: Imbiruçu; MP: Morro do Pão; SI: Serra dos Índios.

Figure 6. Geochemical variation diagrams (major and minor oxides *versus* silica) for MA, IMB, MP and SI granites, showing the composition of samples analyzed in this study compared with literature data.

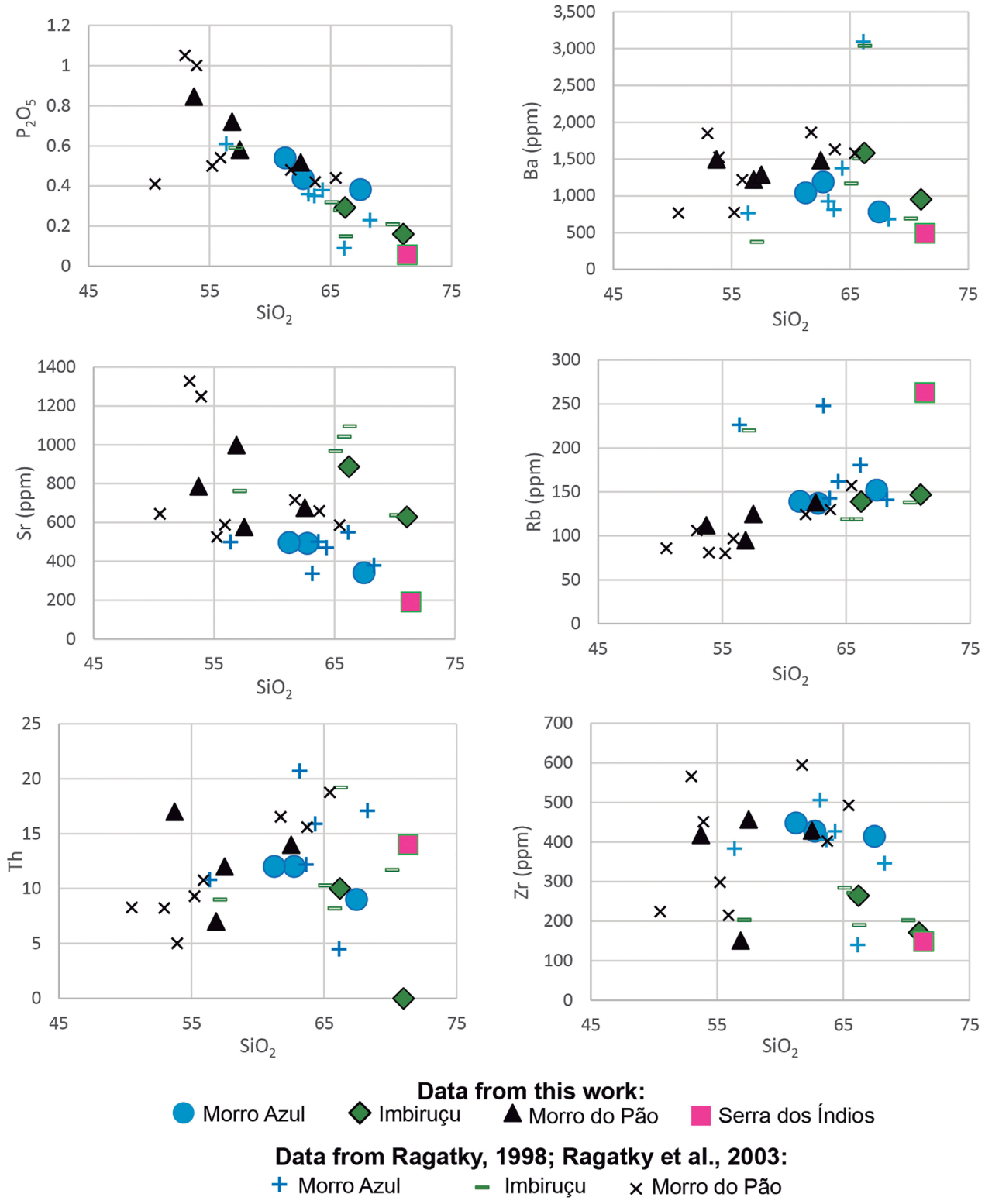

Source: from Ragatky (1998) and Ragatky et al. (2003).
MA: Morro Azul; IMB: Imbiruçu; MP: Morro do Pão; SI: Serra dos Índios.

Figure 7. Geochemical variation diagrams (trace elements *versus* silica) for MA, IMB, MP and SI granites, showing the composition of samples analyzed in this study compared with literature data.

The three most primitive samples of MP (SiO_2 = 54–57 wt.%) are similar to each other; however, a remarkable feature is their higher Al_2O_3 and K_2O and lower CaO and MgO contents compared to the data of Ragatky (1998) for the same occurrence. The reason for the differences is unclear; we consider that they are, at least in part, analytical. Within the set of analyzed samples, IGT-15 is clearly distinguished from the others by lower contents of Zr, Th, Ce and La and higher Sr. Sample IGT-16 is more fractionated and its connection with the typical MP rocks is unclear.

The SI sample has high loss on ignition (LOI) and a very high A/CNK (1.33). The petrographic characteristics are indicative of secondary alteration, especially due to the presence of abundant secondary sericite/muscovite (which may reflect leaching of calcium from plagioclase crystals), and thus its composition must have been altered in relation to the original granite.

ZIRCON AGE DETERMINATION

Results of U-Pb dating of SRD granites (MA, IMB, MP, SI) are shown in Table 3.

Morro Azul Granite

Zircon morphology and U-Pb dating

Zircon crystals (Figure 8) of the MA granite sample IGT-02A are generally elongated, have variable length ranging from 200 to 400 mm, with average size of 290 mm, and average aspect ratio of approximately 4:1 (varying from 3:1 to 6:1). They have medium to high degree of fracturing, well developed oscillatory zoning and occasional inherited nuclei. U contents are 197–662 ppm (median 406 ppm), Th varies from 89 to 243 ppm (median 119 ppm) and the Th/U ratio is typically low, 0.2 to 0.4 (Figure 8).

SHRIMP U-Pb zircon ages were obtained on 14 points, distributed over 11 different crystals. Five of these points correspond to inherited cores. The data (excluding inherited cores) yield concordia age of 601 ± 5 Ma (2s; mean square of weighted deviated (MSWD) = 1.3; probability of concordance = 0.26) for sample IGT-02A (Figure 10).

Three of the inherited nuclei yield results with low discordance (< 4%) and similar $^{207}Pb/^{206}Pb$ ages (2.1–2.2 Ga). The other two results are strongly discordant (34–42%), but are in alignment with those with low discordance; a discordia traced through the results for all inherited crystals has an upper intercept at 2176 ± 21 Ma and lower intercept at the crystallization age of the sample.

Imbiruçu Granite

Zircon morphology and U-Pb dating

The zircon crystals of the Imbiruçu Massif (IGT-23 sample; Figure 8) are generally round, wide (a few are elongated), with lengths varying between 190 and 530 mm, averaging 255 mm; the average aspect ratio is 3:1 (varying from 2:1 to 5:1). They show weak to intermediate degree of fracturing, well developed oscillatory zoning and occasional inherited nuclei. Two groups of crystals can be recognized on the basis of the behavior of Th and U: one with lower Th/U (0.2–0.4), overlapping the compositons of the zircons from MA sample IGT-02A, and a second group with much higher Th/U (0.8–1.3); the two groups follow parallel trends in a Th × U diagram (Figure 9).

SHRIMP age determinations were obtained on 14 spots, distributed over 13 different crystals. Two spots correspond to inherited cores. The data (excluding inherited cores) yielded a concordia age of 606 ± 5 Ma (2s; MSWD = 0.55; probability of concordance = 0.46) for sample IGT-23 (Figure 10).

One of the inherited nuclei shows slightly negative discordance (-4%) and $^{207}Pb/^{206}Pb$ age ~ 1.96 Ga; the other point is strongly discordant (+20%), but clearly has an older age ($^{207}Pb/^{206}Pb$ ~ 2.7 Ga).

Morro do Pão Granite

Zircon morphology and U-Pb dating

Zircon crystals from sample IGT-13 (Figure 8) are elongated, ranging in length from 230 to 380 mm (average 275 mm), and have aspect ratio 4:1 (varying between 3:1 and 5:1). They exhibit very low degree of fracturing, poorly developed oscillatory zoning and do not show signs of inherited nuclei. U and Th contents are low (U, 37–189 ppm, median 68 ppm; Th, 29–268 ppm, median 55 ppm). Th/U varies continuously from 0.6 to 1.2 (Figure 9).

SHRIMP age determination were obtained on 12 spots distributed over 12 different crystals. A concordia age was obtained with 589 ± 5.5 Ma (2s; MSWD = 0.059; probability of concordance = 0.81) (Figure 10).

Serra dos Índios Granite

Zircon morphology and U-Pb dating

Zircon crystals from sample IGT-19 (Figure 8) are generally small, with lengths ranging from 90 to 260 mm (average 230 mm) and a typical aspect ratio of 3:1 (varying from 2:1 to 4:1). They have intermediate to high degree of fracturing, well developed oscillatory zoning and occasional inherited nuclei.

Table 3. Results of U-Pb dating of São Roque Domain (SRD) granites (MA, IMB, MP, SI) by Sensitive High Resolution Ion Micro-Probe (SHRIMP).

Sample spot	Total Pb (common) %	Pb rad ppm	U ppm	Th ppm	Th /U	$^{207}Pb/^{206}Pb$	% err	$^{207}Pb/^{235}U$	% err	$^{206}Pb/^{238}U$	% err	Rho	$^{208}Pb/^{232}Th$	% err	$^{206}Pb/^{238}U$ Age (Ma)	1 s	$^{207}Pb/^{206}Pb$ Age (Ma)	1 s	$^{208}Pb/^{232}Th$ Age (Ma)	1 s	% Discordant
Morro Azul IGT-02A								**UTM S: 7434484 × 380471, 23K**											**concordia age = 601 ± 5 Ma**		
9.1	0.18	16	197	158	0.83	0.05902	2.5	0.771	2.8	0.0947	1.4	0.48	0.0275	2.1	583	8	568	54	549	12	-3
2.1	1.56	32	397	110	0.29	0.06123	3.1	0.803	3.4	0.0951	1.3	0.39	0.0391	5.0	586	7	647	67	776	38	+10
6.1	0.15	32	391	96	0.25	0.05969	1.1	0.796	1.7	0.0967	1.3	0.76	0.0284	2.6	595	7	592	24	566	15	-0
5.1	0.09	23	275	111	0.42	0.05940	1.9	0.800	2.3	0.0977	1.3	0.58	0.0308	2.3	601	8	582	41	614	14	-3
1.1	0.03	33	396	122	0.32	0.05943	1.0	0.802	1.8	0.0979	1.4	0.82	0.0291	2.3	602	8	583	22	579	13	-3
8.1	--	35	414	116	0.29	0.05963	0.9	0.810	1.6	0.0986	1.3	0.83	0.0300	2.2	606	8	590	19	598	13	-3
3.1	0.06	37	434	128	0.30	0.05955	1.0	0.820	1.7	0.0999	1.3	0.78	0.0298	2.4	614	8	587	23	593	14	-5
4.1	0.18	32	366	109	0.31	0.05997	1.3	0.829	1.8	0.1003	1.3	0.72	0.0312	2.6	616	8	602	28	620	16	-2
10.1	--	57	662	243	0.38	0.05983	0.7	0.828	1.4	0.1003	1.3	0.89	0.0317	2.2	616	8	597	14	631	14	-3
7.1 [2]	3.65	63	462	138	0.31	0.09951	0.6	2.256	1.4	0.1644	1.3	0.92	0.0312	2.4	981	12	1,615	11	620	15	+42
7.3	3.62	109	614	106	0.18	0.11085	1.0	3.282	1.8	0.2147	1.5	0.83	0.0337	4.2	1,254	17	1,813	18	669	28	+34
11.1	0.52	185	563	89	0.16	0.13264	0.3	7.019	1.3	0.3838	1.3	0.97	0.1036	2.0	2,094	23	2,133	6	1,993	38	+2
7.2	0.80	87	265	130	0.51	0.13631	0.7	7.275	1.5	0.3871	1.3	0.90	0.1074	1.9	2,109	24	2,181	12	2,061	37	+4
4.2	--	192	537	226	0.44	0.13801	0.3	7.886	1.5	0.4144	1.5	0.99	0.1140	2.0	2,235	28	2,202	4	2,183	41	-2
Imbiruçu IGT-23								**UTM S: 7447862 × 392284, 23K**											**concordia age = 606 ± 5 Ma**		
14.1	0.69	6	81	101	1.29	0.05877	3.9	0.753	4.2	0.0930	1.5	0.37	0.0268	2.7	573	8	559	85	534	14	-3
1.1	0.27	40	485	159	0.34	0.06094	0.8	0.812	1.5	0.0967	1.3	0.84	0.0271	2.0	595	7	637	18	540	11	+7
2.1	0.22	18	219	176	0.83	0.05961	2.6	0.794	3.0	0.0966	1.6	0.52	0.0285	2.2	594	9	589	56	568	12	-1
6.1	0.22	13	155	150	1.00	0.05931	2.0	0.793	2.4	0.0970	1.4	0.58	0.0280	2.3	597	8	579	43	559	12	-3
3.2	0.40	10	113	109	1.00	0.06012	2.5	0.814	2.9	0.0982	1.4	0.50	0.0288	3.4	604	8	608	54	575	19	+1
9.1	0.08	25	295	374	1.31	0.05958	1.2	0.808	1.8	0.0984	1.3	0.74	0.0298	1.6	605	8	588	26	593	10	-3
11.1	0.12	31	360	94	0.27	0.05948	1.2	0.810	1.8	0.0988	1.3	0.74	0.0299	3.5	607	8	585	26	596	21	-4
5.1	0.14	36	420	91	0.22	0.06000	1.5	0.822	2.4	0.0994	1.8	0.77	0.0376	3.5	611	11	604	33	746	25	-1
10.1	0.00	43	505	548	1.12	0.05975	0.8	0.822	1.5	0.0998	1.3	0.85	0.0309	1.6	613	8	595	17	616	9	-3
3.1	--	63	732	226	0.32	0.05968	0.7	0.824	1.4	0.1002	1.3	0.89	0.0319	1.8	615	8	592	15	634	11	-4
7.1	--	36	415	89	0.22	0.05995	1.0	0.843	1.6	0.1020	1.3	0.80	0.0325	4.1	626	8	602	21	646	26	-4
8.1	0.50	15	166	72	0.45	0.06293	2.2	0.926	2.6	0.1067	1.4	0.55	0.0349	3.1	654	9	706	46	693	21	+8
4.1	--	56	176	152	0.89	0.11991	0.5	6.105	1.5	0.3693	1.4	0.93	0.1033	1.6	2,026	24	1,955	10	1,986	30	-4
13.1	5.84	140	421	159	0.39	0.18239	2.3	10.359	3.5	0.4119	2.6	0.74	0.1188	3.7	2,224	49	2,675	39	2,268	78	+20

Continue...

Table 3. Continuation.

Sample spot	Total Pb (common) %	Pb rad ppm	U ppm	Th ppm	Th /U	$^{207}Pb/^{206}Pb$	% err	$^{207}Pb/^{235}U$	% err	$^{206}Pb/^{238}U$	% err	Rho	$^{208}Pb/^{232}Th$	% err	$^{206}Pb/^{238}U$ Age (Ma)	1 s	$^{207}Pb/^{206}Pb$ Age (Ma)	1 s	$^{208}Pb/^{232}Th$ Age (Ma)	1 s	% Discordant
Morro do Pão IGT-13										**UTM S: 7449479 × 386787, 23K**							**concordia age = 589 ±5.5 Ma**				
12.1	0.54	8	101	66	0.67	0.05902	3.3	0.745	3.6	0.0915	1.5	0.41	0.0272	3.5	565	8	568	72	542	19	+1
10.1	1.48	4	51	58	1.18	0.05903	7.8	0.750	8.0	0.0921	1.7	0.21	0.0286	3.8	568	9	568	171	570	21	+0
7.1	1.84	5	57	42	0.77	0.06045	6.8	0.786	7.2	0.0943	2.3	0.32	0.0294	5.4	581	13	620	147	585	31	+7
3.1	1.38	6	70	77	1.13	0.06015	8.0	0.785	8.2	0.0947	1.6	0.20	0.0284	4.5	583	9	609	174	566	25	+4
11.1	0.32	4	44	39	0.92	0.06058	8.7	0.794	8.9	0.0951	1.7	0.20	0.0298	3.7	585	10	624	188	594	21	+7
4.1	0.33	12	143	268	1.94	0.05936	2.4	0.783	2.8	0.0957	1.4	0.52	0.0283	1.9	589	8	580	51	565	11	-2
2.1	0.64	12	145	96	0.68	0.06026	2.6	0.797	3.0	0.0959	1.4	0.48	0.0266	4.4	590	8	613	56	531	23	+4
1.1	2.25	3	37	38	1.06	0.05991	9.2	0.795	9.4	0.0962	1.9	0.20	0.0270	6.6	592	11	600	200	538	35	+1
5.1	0.84	6	77	53	0.71	0.05945	4.5	0.789	4.8	0.0962	1.6	0.33	0.0283	5.9	592	9	583	98	564	33	-2
9.1	0.07	16	189	29	0.16	0.05963	1.5	0.797	2.1	0.0969	1.4	0.67	0.0304	4.4	596	8	590	33	605	27	-1
6.1	2.14	5	66	72	1.14	0.06110	7.6	0.819	7.7	0.0972	1.6	0.21	0.0306	3.7	598	9	643	162	608	22	+7
8.1	0.62	3	40	46	1.19	0.06033	5.2	0.811	5.5	0.0974	1.8	0.32	0.0295	3.7	599	10	616	113	587	22	+3
Serra dos Índios IGT-19										**UTM S: 7455650 × 392132, 23K**							**concordia age = 593 ±12 Ma**				
4.1 (1)	7.93	15	209	70	0.34	0.06551	13.1	0.750	13.2	0.0830	1.7	0.13	0.0290	12.4	514	8	791	274	578	70	+36
5.2	3.65	23	316	131	0.43	0.06240	6.8	0.743	6.9	0.0864	1.4	0.20	0.0300	5.1	534	7	688	145	597	30	+23
4.2	1.96	6	76	59	0.80	0.06140	6.4	0.740	6.6	0.0874	1.6	0.24	0.0293	4.1	540	8	653	138	584	24	+18
10.1 (1)	7.31	23	295	101	0.35	0.06332	8.4	0.787	8.5	0.0901	1.5	0.17	0.0293	10.4	556	8	719	179	584	60	+24
3.2 (1)	29.61	51	641	238	0.38	0.07724	23.2	1.000	23.3	0.0939	2.2	0.10	0.0517	17.7	579	12	1,127	462	1019	176	+51
7.1	4.81	37	463	210	0.47	0.06608	3.9	0.847	4.2	0.0929	1.5	0.37	0.0325	5.0	573	8	809	82	646	32	+30
11.1	0.69	14	167	100	0.62	0.06001	2.7	0.783	3.1	0.0946	1.4	0.46	0.0282	3.1	583	8	604	59	563	17	+4
5.1	5.58	16	192	66	0.35	0.06023	7.8	0.789	7.9	0.0950	1.5	0.19	0.0297	10.3	585	8	612	168	591	60	+5
12.1	0.85	5	55	85	1.58	0.06028	4.7	0.810	5.0	0.0975	1.7	0.33	0.0286	3.0	600	9	613	101	570	17	+2
8.1	0.82	21	249	1,171	4.86	0.06050	2.2	0.815	2.6	0.0978	1.3	0.52	0.0294	1.5	601	8	622	48	586	9	+3
6.1	0.53	6	70	126	1.85	0.06059	5.2	0.850	5.5	0.1018	1.6	0.29	0.0298	2.5	625	9	625	113	593	15	-0
9.1	1.11	8	89	96	1.11	0.06126	4.7	0.864	4.9	0.1023	1.5	0.31	0.0343	3.0	628	9	648	100	682	20	+3
3.1	5.05	77	746	590	0.82	0.06322	6.5	1.041	8.4	0.1195	5.3	0.63	0.0540	6.3	727	37	716	138	1,063	65	-2
1.1 (1)	9.70	37	181	77	0.44	0.12713	2.7	4.384	5.4	0.2501	4.7	0.87	0.0832	7.5	1,439	60	2,059	47	1,615	116	+34
2.1	0.68	58	190	71	0.39	0.12681	0.5	6.305	1.4	0.3606	1.4	0.95	0.0996	2.4	1,985	23	2,054	8	1,920	45	+4

U and Th contents vary widely (U, 70–746 ppm, median = 192 ppm; Th, 59–1,171 ppm, median 100 ppm). Many crystals have Th/U within a small range (0.3–0.5), but U-poor spots have Th/U up to 1.8 (Figure 9).

SHRIMP age determinations were obtained on 15 points distributed over 12 different crystals. The data (excluding inherited cores and results with high common Pb) yield a concordia age of 593 ± 12 Ma (2s; MSWD = 2.2; probability of concordance = 0.14), therefore with greater uncertainty when compared to the ages obtained for the other plutons (Figure 10).

Inherited core 2.1 has low discordance (4%), while 1.1 is strongly discordant (34%); however, their $^{207}Pb/^{206}Pb$ ages are identical (~ 2.05 Ga).

DISCUSSION

Age of granite magmatism in eastern São Roque Domain

Recent SHRIMP and LA-ICPMS U-Pb zircon age determinations for the main granite occurrences at the central portion

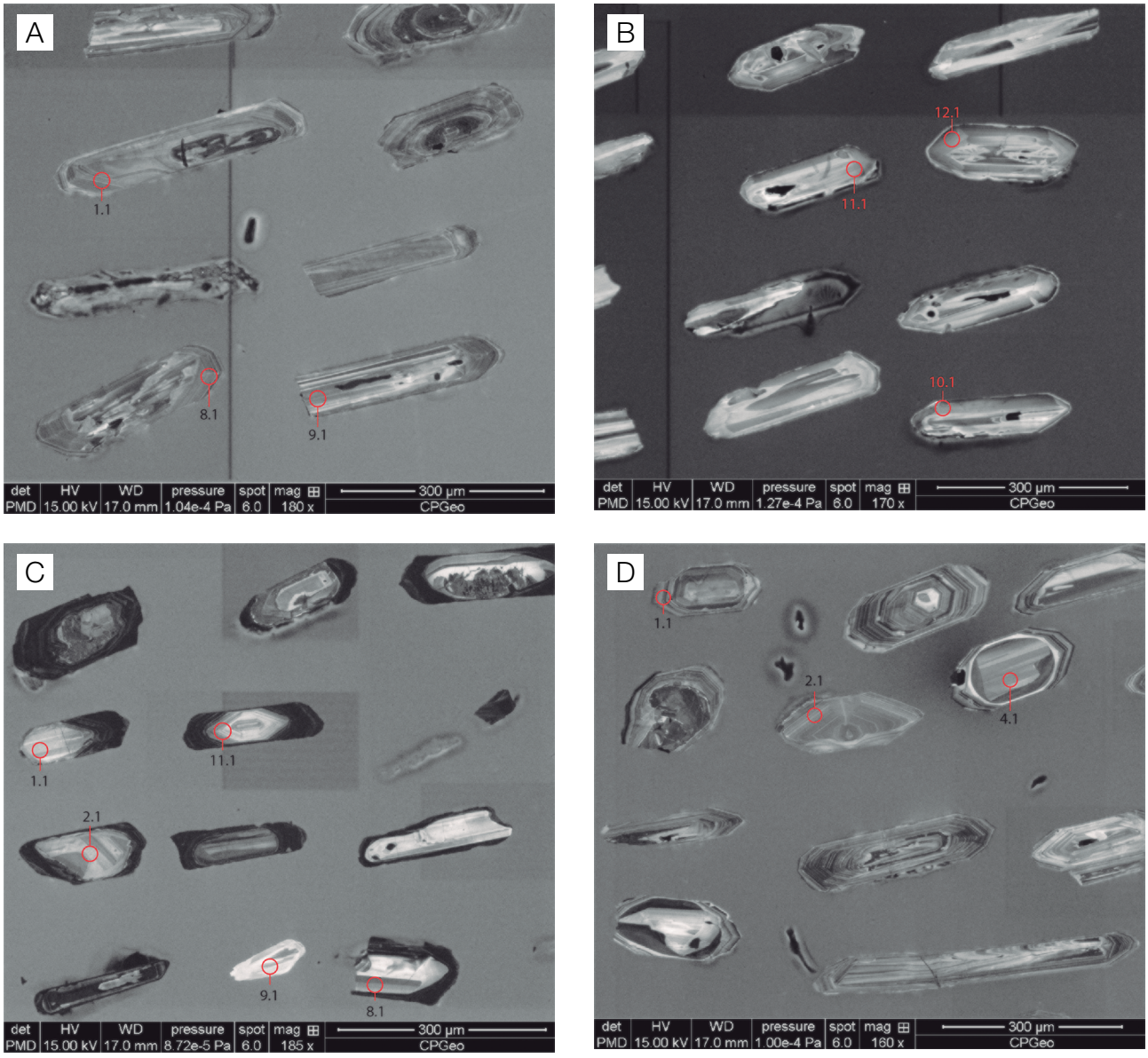

Figure 8. Cathodoluminescence images of selected zircon grains from samples of (A) Morro Azul granite; (B) Morro do Pão tonalite; (C) Serra dos Índios leucogranite; and (D) Imbiruçu granite. Numbers and circles indicate position of analyzed spots.

of SRD have indicated a short peak of granitic magmatism between 604 ± 3 Ma and 590 ± 4 Ma. Moreover, the predominant high-K calc-alkaline magmatism was shown to spread over the oldest ~10 Ma range, and other types with peraluminous and subalkaline character were restricted to the 590–592 Ma interval (Janasi et al., 2016).

The SHRIMP UPb zircon data presented here suggest that the granite magmatism in the eastern portion of SRD

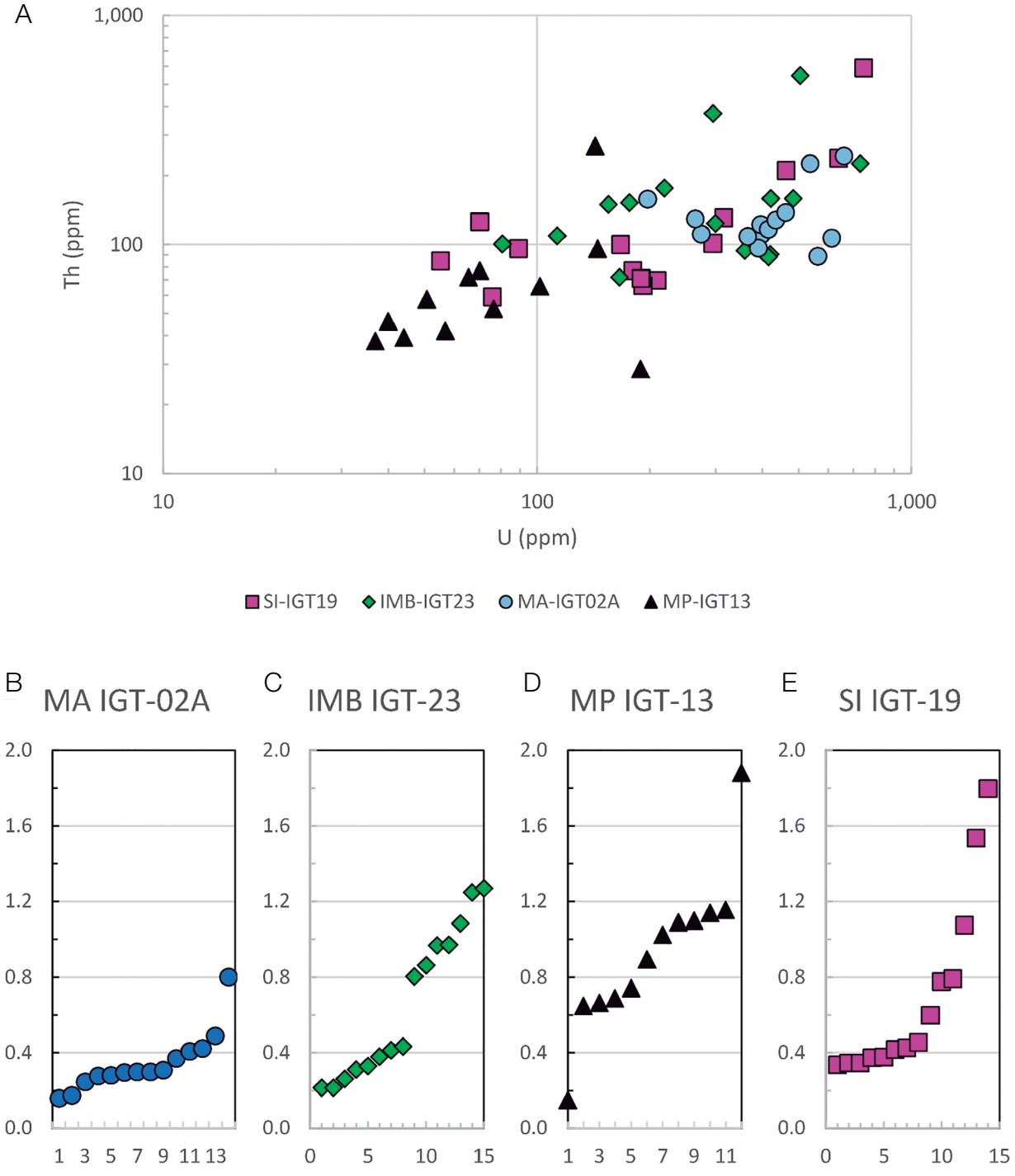

Figure 9. Th and U composition of dated zircon crystals of granites from the eastern São Roque Domain (SRD): (A) Th × U variation; (B to E): range of Th/U variation in individual samples.

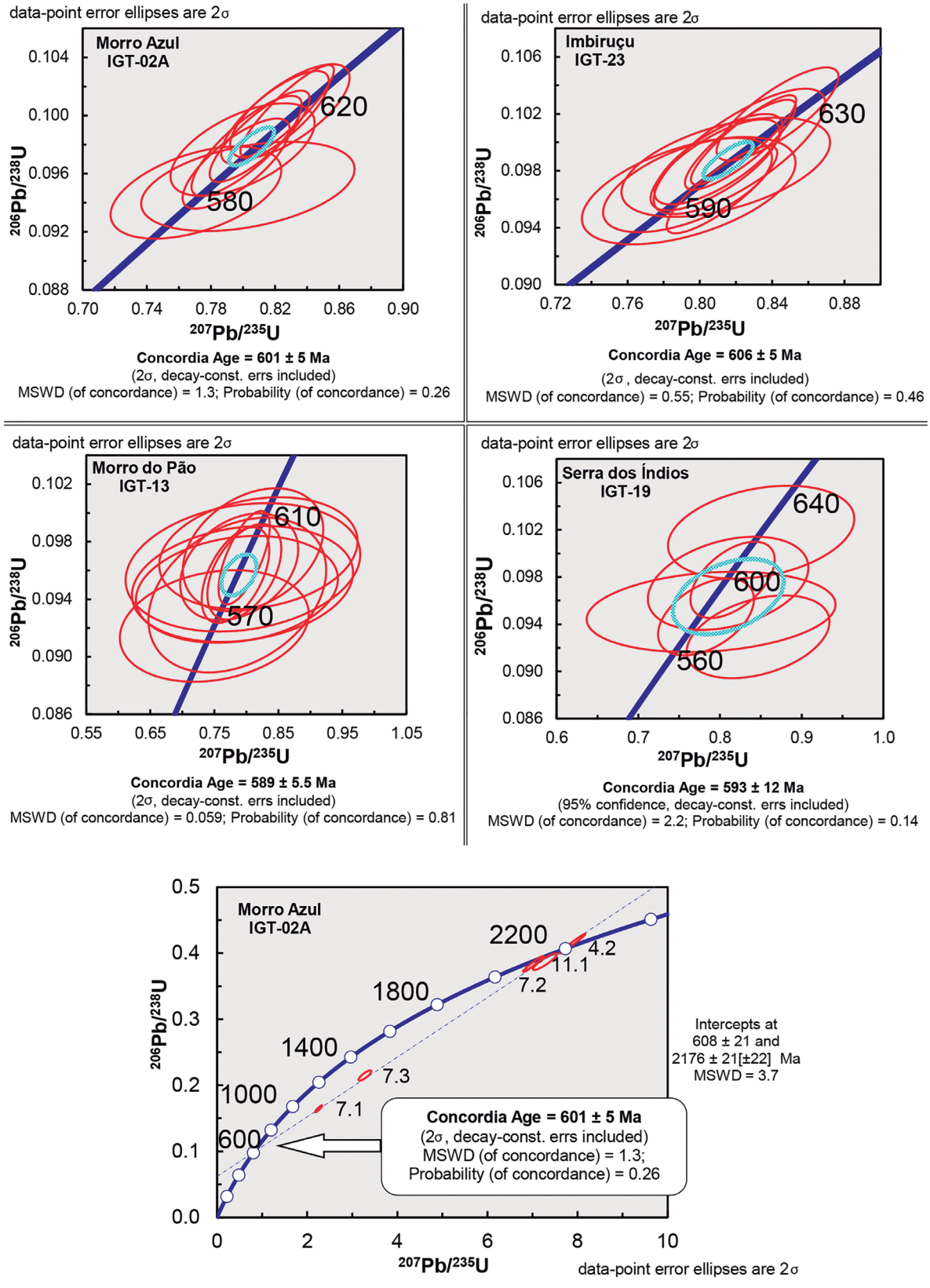

Figure 10. U-Pb isotope diagrams showing results of *in situ* zircon dating by Sensitive High Resolution Ion Micro-Probe (SHRIMP).

occurred essentially within the same age interval, confirming also that the high-K calc-alkaline plutons (MA and IMB) are slightly older (606–601 Ma) than other types (represented here by the mafic-rich MP tonalite dated at 589.1 ± 5.5 Ma and the SI peraluminous leucogranite at 593 ± 12 Ma) (Figure 11).

Previous estimates of the age of granites from the eastern SRD were restricted to Rb-Sr isotope data presented by Ragatky et al. (2003) for MA and IMB granites. High uncertainties (~20 Ma) were associated with these results, and the age assigned to the MA granite (532 ± 20 Ma) appeared too young. Our new U-Pb zircon ages overcome these limitations and yield more reliable estimates for the crystallization ages of these plutons that are consistent with the regional framework.

Implications to the petrogenesis of the SRD granites

Although the focus of the present work is on the precise determination of the ages of granite plutons from the eastern SRD, the new geochemical and zircon inheritance data presented here bring some important information bearing on the petrogenesis of these granites.

The MA and IMB plutons are aligned along the southern portion of the SRD, close to and in part affected by the Taxaquara Shear Zone. The geometry of the MA granite, which has a penetrative solid-state foliation over its entire length, is clearly controlled by this fault zone, while the IMB granite has a more ellipsoidal shape in plant, and is elongated in the same direction. Both plutons are constituted by monzogranites with similar porphyritic texture, bearing large, abundant alkali feldspar megacrysts, and frequent microgranular enclaves with color indices slightly higher than the host granite. The main field distinctions are the presence of a more felsic variety the IMB pluton and the

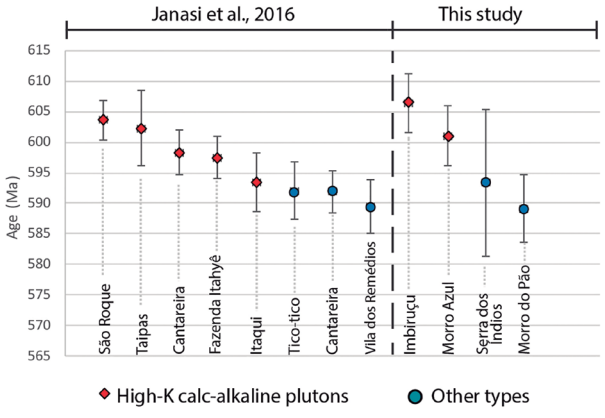

Figure 11. Comparison between data from Janasi et al. (2016) and data from this study for age granite magmatism in plutons of the eastern portion of São Roque Domain (SRD).

systematically low magnetic susceptibility shown by MA granites and enclaves, indicative of the absence or scarcity of magnetite and thus a more reduced character.

A genetic relationship between the two plutons may be thus considered, and the more reduced character of MA could be attributed to assimilation of reduced country-rock metasediments, as inferred for similar plutons (e.g., the Mauá granite in the Embu Domain; Alves et al., 2009). Indeed, some geochemical affinities between the two plutons are evident, and could support this interpretation. However, important differences are seen in the contents of some elements. A closer examination of the variation diagrams shows that, for similar degrees of differentiation, the MA granite has lower contents of K, Al, Ba, Sr and higher Fe, Ti, Mn, P, Zr, Nb contents when compared to IMB. A difference in Sr and Zr contents (Sr/Zr = 0.8–1.2 for MA and 3.3–3.7 for IMB) is particularly remarkable and is not consistent with a simple comagmatic relationship between the two plutons. The high Sr and relatively low Zr contents of the IMB granites are more typical of the high-K calc-alkaline granites found in the central portion of the SRD (see for instance the data presented by Janasi et al., 2016), which may be characterized as high Ba-Sr granites. As pointed out by Janasi et al. (2016), the high Sr contents and discreet to absent negative Eu anomalies in the REE patterns of these granites may be related to their origin in deep seated (lower crustal?) sources where garnet is the stable phase in place of plagioclase. The IMB granites, on the other hand, do not share this signature, which implies different sources and/or melting conditions at the same age.

Inherited zircons are present in all dated samples, with the exception of the more mafic (and thus supposedly hotter) MP tonalite. It is remarkable that all have similar ages (> 2.0 Ga, and concentrated in the 2.0–2.2 Ga range), which coincides with the inheritance pattern of granite occurrences of the central SRD (Janasi et al., 2016) and with the age peak of detrital zircons from metasediments of this domain (Henrique-Pinto et al., 2015). As indicated by the Nd isotope data presented by Ragatky (1998), Sm-Nd depleted mantle ages as low as 1.4 Ga are present in granites from the eastern SRD; thus far, the inherited zircon data do not indicate the presence of crust younger than 2.0 Ga in their source. Lowering of the model ages by a Neoproterozoic mantle component is a possibility that should be evaluated, and is reinforced by their occurrence in the primitive MP tonalites.

CONCLUSIONS

U-Pb SHRIMP zircon dating of four granitic plutons of varied composition from the easternmost portion of SRD indicates that the peak of granitic magmatism in that region was concentrated in a short interval between 606

and 589 (±5) Ma, the same interval identified in the central portion of the domain. The two occurrences of porphyritic biotite granite (Morro Azul and Imbiruçu) yield the oldest ages, identical within error (respectively, 601.0 ± 4.9 Ma and 606.3 ± 4.8 Ma) and have inherited zircons with the same age (~2.1–2.0 Ga), but do not seem to be related through simple fractionation-contamination processes. The IMB granites have geochemical signature similar to other typical SRD HKCA granites (e.g., high Sr, high Ce/Y), partly modified by assimilation of metasedimentary rocks. Morro Azul, on the other hand, has consistently lower Sr and higher Zr, which demands contemporaneous mobilization of a different source.

The compositions of the other two dated occurrences are very different from each other and from the MA and IMB granites. The age obtained for the MP tonalite (589.1 ± 5.5 Ma) clearly indicates that, in spite of its more deformed character, it is younger than MA and IMB. A similar value, although with large uncertainty, was determined for the SI peraluminous leucogranite (593 ± 12 Ma). Together with available geochronological data from the central part of the SRD, this indicates that soon after the main episode of HKCA magmatism, the SRD witnessed the emplacement of granites of widely varied composition (tonalites, leucogranites, subalkaline granites) in the form of small bodies which record strong deformation related to transcurrent tectonics.

ACKNOWLEDGEMENTS

We acknowledge Fundação de Amparo à Pesquisa do Estado de São Paulo (FAPESP) for financial support (grant 2015/01817-6 to VAJ and scholarship 2016/16418-2 to ISML). We also appreciate qualified support from Geoanalitica technical staff for chemical analysis and from the CPGeo, especially Kei Sato, for support during analytical work and interpretation of SHRIMP data.

REFERENCES

Almeida, F.F.M., Hasui, Y., Brito Neves, B.B., Fuck, R.A. (1981). Brazilian structural provinces: An introduction. *Earth-Science Reviews*, 17, 1-29. https://doi.org/10.1016.0012-8252(81)90003-9

Alves, A., Janasi, V. D. A., Simonetti, A., Heaman, L. (2009). Microgranitic Enclaves as Products of Self-mixing Events: a Study of Open-system Processes in the Maua Granite, Sao Paulo, Brazil, Based on in situ Isotopic and Trace Elements in Plagioclase. *Journal of Petrology*, 50(12), 2221-2247. https://doi.org/10.1093/petrology/egp074

Black, L. P., Kamo, S. L., Allen, C. M., Davis, D. W., Aleinikoff, J. N., Valley, J. W., Mundil, R., Campbell, I. H., Korsch, R. J., Williams, I. S., Foudoulis, C. (2004). Improved 206Pb/238U microprobe geochronology by the monitoring of a trace-element-related matrix effect; SHRIMP, ID–TIMS, ELA–ICP–MS and oxygen isotope documentation for a series of zircon standards. *Chemical Geology*, 205(1-2), 115-140. https://doi.org/10.1016/j.chemgeo.2004.01.003

Campanha, G. A. C., Faleiros, F. M., Cawood, P. A., Cabrita, D. I. G., Ribeiro, B. V., Basei, M. A. S. (2019). The Tonian Embu Complex in the Ribeira Belt (Brazil): revision, depositional age and setting in Rodinia and West Gondwana. *Precambrian Research*, 320, 31-45. https://doi.org/10.1016/j.precamres.2018.10.010

Campos Neto, M. C. (2000). Orogenic systems from Southwestern Gondwana: An approach to Brasiliano-Pan-African cycle and orogenic collage in Southeastern Brazil. *In*: U. G. Cordani, E. J. Milani, A. Thomaz Filho, D. A. Campos (Eds.). Tec*tonic Evolution of South America* (355-365). Rio de Janeiro, 31st International Geological Congress.

Campos Neto, M. C., Basei, M. A. S., Artur, A. C., Silva, M. E., Machado, R., Dias Neto, C .M., Fragoso-Cesar, A. R., Souza, A. P. (1983). *Geologia das Folhas Piracaia e Igaratá*. 1ª Jornada sobre a Carta Geológica do Estado de São Paulo em 1:50.000. São Paulo: Pró-Minério, p. 55-76.

Campos Neto, M. C., Cioffi, C. R., Moraes, R., Motta, R. G., Siga Jr., O., Basei, M. A. S. (2010). Structural and metamorphic control on the exhumation of high-P granulites: The Carvalhos Klippe example, from the oriental Andrelândia Nappe System, southern portion of the Brasília Orogen, Brazil. *Precambrian Research*, 180(3-4), 125-142. https://doi.org/10.1016/j.precamres.2010.05.010

Duffles, P., Trouw, R. A. J., Mendes, J. C., Gerdes, A., Vinagre, R. (2016). U–Pb age of detrital zircon from the Embu sequence, Ribeira belt, Se Brazil. *Precambrian Research*, 278, 69-86. https://doi.org/10.1016/j.precamres.2016.03.007

Hackspacher, P. C., Dantas, E. L., Spoladore, A., Fetter, A. H., Oliveira, M. A. F. (2000). Evidence of neoproterozoic backarc basin development in the Central Ribeira Belt, southeastern Brazil: new geochronological and geochemical contraints from the São Roque-Açungui groups. *Revista Brasileira de Geociências*, 30(1), 110-114. https://doi.org/10.25249/0375-7536.2000301110114

Henrique-Pinto, R., Janasi, V. A., Campanha, G. A. C. (2018). U-Pb dating, Lu-Hf isotope systematics and chemistry of zircon from the Morro do Polvilho meta-trachydacite: constraints on sources of magmatism and on the depositional age of the São Roque Group. *Geologia USP. Série Científica*, 18(2), 45-56. https://doi.org/10.11606/issn.2316-9095.v18-125793

Henrique-Pinto, R., Janasi, V. A., Vasconcellos, A. C. B. C., Sawyer, E. W., Barnes, S. J., Basei, M. A. S., Tassinari, C. C. G. (2015). Zircon provenance in meta-sandstones of the São Roque Domain: Implications for the Proterozoic evolution of the Ribeira Belt, SE Brazil. *Precambrian Research*, 256, 271-288. https://doi.org/10.1016/j.precamres.2014.11.014

Janasi, V. A., Andrade, S., Vasconcellos, A. C. B. C., Henrique-Pinto, R., Ulbrich, H. H. G. J. (2016). Timing and sources of granite magmatism in the Ribeira Belt, SE Brazil: Insights from zircon in situ U–Pb dating and Hf isotope geochemistry in granites from the São Roque Domain. *Journal of South American Earth Sciences*, 68, 224-247. https://doi.org/10.1016/j.jsames.2015.11.009

Juliani, C., Hackspacher, P. C., Dantas, E. L., Fetter, A. H. (2000). The Mesoproterozoic volcano-sedimentary Serra do Itaberaba Group of the Central Ribeira Belt, São Paulo State, Brazil: implications for the age of the overlying São Roque Group. *Revista Brasileira de Geociências*, 30(1), 82-86. https://doi.org/10.25249/0375-7536.2000301082086

Ludwig, K. R. (2003). *User's manual for Isoplot 3.00: a geochronological toolkit for Microsoft Excel.* Berkeley: Berkeley Geochronology Center, Special Publication, n. 4.

Ludwig, K. R. (2009). *User's manual for SQUID 2.* Berkeley: Berkeley Geochronology Center, Special Publication.

Mori, P. E., Reeves, S., Correia, C. T., Haukka, M. (1999). Development of a fused glass disc XRF facility and comparison with the pressed powder pellet technique at Instituto de Geociências, Universidade de São Paulo. *Revista Brasileira de Geociências*, 29(3), 441-446. https://doi.org/10.25249/0375-7536.199929441446

Ragatky, C. D. (1998). *Contribuição à geoquímica e geocronologia do Domínio São Roque e da Nappe de Empurrão Socorro-Guaxupé na região de Igaratá e Piracaia, SP*. Thesis (Doctoral). São Paulo: Instituto de Geociências – USP, 131 p. https://doi.org/10.11606/T.44.2016.tde-12012016-153236

Ragatky, C. D., Duarte, B. P., Tassinari, C. (2013). Caracterização geoquímica e isotópica de granitóides do domínio São Roque, Faixa Ribeira, São Paulo. *Revista de Ciências Exatas*, 22(1-2), 57-72.

Sato, K., Tassinari, C. C. G., Basei, M. A. S., Siga Jr., O., Onoe, A. T., Souza, M. D. (2014). Sensitive High Resolution Ion Microprobe (SHRIMP IIe/MC) of the Institute of Geosciences of the University of São Paulo, Brazil: analytical method and first results. *Geologia USP. Série Científica*, 14(3), 3-18. https://doi.org/10.5327/Z1519-874X201400030001

Stacey, J. S., Kramers, J. D. (1975). Approximation of terrestrial lead isotope evolution by a two-stage model. *Earth and Planetary Science Letters*, 26(2), 207-221. https://doi.org/10.1016/0012-821X(75)90088-6

Töpfner, C. (1996). Brasiliano-granitoide in den Bundesstaaten São Paulo und Minas Gerais, Brasilien: eine vergleichende Studie. *In*: C. Töpfner, ed. *Münchner Geologische Hefte*. Germany: Inst. für Allg. und Angewandte Geologie. v. 17, 258 p.